LA-UR-11-04886

Approved for public release;
distribution is unlimited.

Title:	Temperature Effects of Resonance Scattering in Free Gas for Epithermal Neutrons
Author(s):	Eva E. Sunny, Forrest B. Brown, Brian C. Kiedrowski, William R. Martin
Intended for:	MCNP References

Los Alamos National Laboratory, an affirmative action/equal opportunity employer, is operated by the Los Alamos National Security, LLC for the National Nuclear Security Administration of the U.S. Department of Energy under contract DE-AC52-06NA25396. By acceptance of this article, the publisher recognizes that the U.S. Government retains a nonexclusive, royalty-free license to publish or reproduce the published form of this contribution, or to allow others to do so, for U.S. Government purposes. Los Alamos National Laboratory requests that the publisher identify this article as work performed under the auspices of the U.S. Department of Energy. Los Alamos National Laboratory strongly supports academic freedom and a researcher's right to publish; as an institution, however, the Laboratory does not endorse the viewpoint of a publication or guarantee its technical correctness.

Form 836 (7/06)

TEMPERATURE EFFECTS OF RESONANCE SCATTERING IN FREE GAS FOR EPITHERMAL NEUTRONS

Eva E. Sunny[1], Forrest B. Brown[2], Brian C. Kiedrowski[2], William R. Martin[1]

[1]The University of Michigan – Ann Arbor
Department of Nuclear Engineering & Radiological Sciences
2355 Bonisteel Blvd, Ann Arbor, MI 48109
esunny@umich.edu, wrm@umich.edu

[2]Los Alamos National Laboratory
X-Computational Physics Division, Monte Carlo Codes Group
Los Alamos, NM 87545
fbrown@lanl.gov, bckiedro@lanl.gov

Table of Contents

Table of Tables

Table of Figures

1 SUMMARY

The double-integral equation for effective neutron scattering cross section with target nuclide thermal motion can be integrated analytically if one assumes constant scattering cross section instead of assuming cross section dependence on relative neutron speed. Therefore, integrating the double-integral equation to determine the effective neutron scattering cross section was simplified in the past by using constant scattering cross sections and Maxwell-Boltzmann distribution for target atoms. The target atoms are assumed to be unbound, ignoring any molecular or crystalline effects. Assuming constant scattering cross sections in the epithermal range is reasonable for many applications because light nuclides have nearly constant cross sections in the epithermal energy range. However, moderation due to scatter off heavy nuclides is often negligible, thus justifying the use of constant scattering cross sections even for heavy nuclides. Since the scattering cross section was considered to be constant, the bivariate probability density function (PDF) for scattering also depended on using constant scattering cross sections.

Based on these simplifying assumptions, it was still not possible to analytically determine target atom speed and cosine of polar angle from the bivariate PDF without using a rejection technique or constructing the CDF for all incident neutron energies from a discretized PDF to sample for atom speed and angle. The latter method is computationally expensive and was not feasible to implement before the days of High-Performance Computers (HPC). A Monte Carlo scheme that involves a rejection technique proposed by H. Kahn [1] is used to implement the free gas scattering kernel in MCNP [2] to sample target atom speed and cosine of polar angle between the neutron and target atom. The free gas scattering kernel is activated in MCNP when target atoms have a temperature of less than 400kT (MeV) where k is the Boltzmann constant and T is the temperature of the target.

The original free gas scattering kernel accounts for target atom motion in the epithermal range, but the simplifying assumption of using constant scattering cross sections does not correctly take into account the double-differential scattering kernel for neutron scatter, especially off heavy nuclides. Recent studies by M. Ouisloumen *et. al.* [3], W. Rothenstein *et. al.* [4], B. Becker *et. al.* [5] and D. Lee *et. al.* [6] have shown that when cross section dependence on relative neutron speed is taken into account, resonance scattering off heavy nuclides can cause the neutron to gain speed with greater likelihood than previously considered with the use of constant scattering cross sections in the free gas scattering kernel. This meant in heavy nuclides, neutrons could potentially fall back into an absorption resonance with greater probability after slowing down past a resonance, leading to the conclusion that scattering cross section dependence on relative speed of the neutron cannot be ignored for heavy nuclides.

This work done in resonance scattering raises an issue about the type of scattering kernel to be used in the epithermal energy range in reactor calculations. Deterministic codes use the asymptotic scattering kernel where the target is assumed to be at rest. Papers published on resonance scattering show that the physical behavior where neutrons gain speed due to target atom motion in the epithermal range show noticeable differences in criticality calculations and cannot be disregarded [3], [5], [6]. The use of the original free gas scattering kernel proposed by H. Kahn [1] takes into account some neutron up-scatter in MCNP, but it is important to use cross sections dependent on relative neutron speed to correctly account for neutron scattering effects. The use of HPCs facilitate faster and more accurate Monte Carlo calculations with large number of particles and cycles, and the effects of the assumptions in the current free gas scattering kernel are now evident and are no longer in the noise range. Very High Temperature Reactor (VHTR) calculations seem to be affected the most by this phenomenon, which is dependent on fuel packing fraction, fuel temperature and fuel enrichment. Criticality calculations for VHTRs can vary on the order of several hundred per cent mille (pcm), approximately one dollar of reactivity, because of resonances lying in the lower epithermal energy range in U-238.

The Doppler Broadening Rejection Correction (DBRC) method proposed by B. Becker *et. al.* [5] is implemented in MCNP5. This method is selected over other methods for implementation in MCNP5 since it is based on the free gas scattering kernel on which MCNP5 currently operates. The DBRC method is implemented and benchmark calculations are performed, the results of which are outlined in detail.

2 BACKGROUND

Several methods account for neutrons slowing down in capturing media with target nuclides in thermal motion. These methods, however, focus on changing the integral equations to differential equations and using numerical methods to solve the integral equations. One of the main assumptions used in these models is that the scattering cross sections remain constant, thereby simplifying the calculations. Coveyou *et. al*. [1] presented a Monte Carlo method proposed by H. Kahn [1] to sample for target atom speed and cosine of polar angle to form the well known free gas scattering kernel, which is implemented in MCNP5-1.60.

Marchuk *et. al.* [7], and Blackshaw *et. al.* [8] focused on approximating the differential scattering probability for cross sections that are not constant using Legendre expansions to calculate the moments. M. Ouisloumen *et. al.* [3] also used Legendre expansions to calculate the differential scattering probability using the zeroth moment for cross sections that are a function of relative speed of the neutron. They showed that it is possible for the neutron to gain energy off a scatter with a heavy nuclide only to fall into an absorption resonance to be absorbed in the epithermal range. This effect was shown to be more prominent as the temperature of the system increased. Resonance up-scattering effects are therefore considered to be more important in VHTRs and in Light Water Reactors (LWRs) because they are shown to affect criticality calculations on the order of several hundred pcm depending on the enrichment of the fuel, packing fraction and temperature of the fuel.

B. Becker *et. al.* [5] modified the free gas scattering kernel proposed by H. Kahn to account for up-scattering effects and this method is discussed in more detail in the following sections. D. Lee *et. al.* [6] discretized the bivariate PDF for scattering, to sample for the target atom speed and the cosine of polar angle. However, they found that calculating the PDF and subsequently the cumulative distribution function (CDF) to sample for cosine of polar angle and speed of the target atom for incident neutron energy after every single scatter was computationally expensive. Later, they implemented an accelerated scheme where they assigned the neutron a weight as shown,

$$w_{i+1} = w_i \frac{\sigma_t\left(v_r\right)\frac{v_r}{v'} + \sigma_b}{\sigma_t^{eff}\left(v'\right)\frac{v_r}{v'} + \sigma_b},$$

where σ_t is the total cross section, σ_t^{eff} is the effective total cross section, σ_b is the background cross section, v_r is the relative neutron speed and v' is the incident neutron speed.

D. Lee *et. al.* [6] obtained results comparable to B. Becker *et. al.* [5] and M. Ouisloumen *et. al.* [3]. T. Mori *et. al.* [9] also developed a similar method and applied a correction factor for the neutron weight shown,

$$f = \frac{\sigma_s\left(v_r\right)}{\sigma_s^{eff}\left(v'\right)},$$

where σ_s is the scattering cross section and σ_s^{eff} is the effective scattering cross section.

Their results are also comparable to results published by D. Lee *et. al.* [6]. This work showed the importance of accounting for resonance scattering in reactor calculations and illustrated the need to account for resonance scattering in MCNP.

3 FREE GAS SCATTERING TREATMENT

The free gas scattering treatment requires two assumptions. The first is that the moderating and absorbing atoms are unbound to ignore any molecular and crystalline effects. Second, the unbound atoms are in a Maxwell-Boltzmann distribution in energy.

Eq. (1) is the starting point for the derivation of effective scattering cross section because the double-integral equation represents the integration of the probability of neutron collision per second over all polar and azimuthal angles, and target atom speed,

$$\Sigma_{eff,s}(v)=\int_{4\pi}\int_{0}^{\infty}\frac{|\mathbf{v}-\mathbf{V}|}{v}N\sigma_s(|\mathbf{v}-\mathbf{V}|)P(\mathbf{V})d\mathbf{V}\,d\Omega\ , \tag{1}$$

$$where,\ P(\mathbf{V})=\left(\frac{M}{2\pi kT}\right)^{\frac{3}{2}}e^{-\left(M/2kT\right)\mathbf{v}^2}\ .$$

v is neutron velocity and **V** is target nuclide velocity, both of which are in laboratory system.

If σ_s is assumed to be constant, then after performing several manipulations to Eq. (1), the following equation for the effective scattering cross section of a neutron in free gas is derived,

$$\Sigma_{eff,s}(v)=N\sigma_s\left[\frac{e^{-\alpha v^2}}{v\sqrt{\pi\alpha}}+\left(1+\frac{1}{2\alpha v^2}\right)erf\left(v\sqrt{\alpha}\right)\right], \tag{2}$$

$$where,\ \alpha=\frac{M}{2kT}.$$

Neutron scattering in a system depends on the speed of the target atom and the direction of motion of the neutron with respect to the target atom. Both these variables can be used to calculate the relative speed of the neutron in the system. This means that the neutron probability of scatter is a bivariate PDF. Therefore, the two variables, atom speed, and cosine of polar angle between the neutron and target atom for a given incident neutron velocity are factors in this bivariate PDF (assuming σ_s is constant):

$$P(V,\mu\,|\,v)dV\,d\mu=\frac{N\left(\frac{\alpha}{\pi}\right)^{3/2}\sigma_s\,|\mathbf{v}-\mathbf{V}|\,V^2e^{-\alpha V^2}2\pi\,dV\,d\mu}{\Sigma_{eff,s}\left(v\right)}\ . \tag{3}$$

Directly sampling from the bivariate PDF is complicated due to the presence of relative speed. H. Kahn [1] recommended a method to overcome the direct sampling problem by suggesting a rejection method to determine the choices of the target atom speed and cosine of polar angle. The method involves factoring Eq. (3) into the form:

$$P\left(V,\mu\,|\,v\right)dV\,d\mu=\frac{1}{\Sigma_{eff,s}\left(v\right)}\begin{bmatrix}4\pi N\left(\frac{\alpha_s}{\pi}\right)^{3/2}\sigma_s vV^2e^{-\alpha_s V^2}dV\frac{d\mu}{2}+\ldots\\ \ldots 4\pi N\left(\frac{\alpha_s}{\pi}\right)^{3/2}\sigma_s V^3e^{-\alpha_s V^2}dV\frac{d\mu}{2}\end{bmatrix}\frac{|\mathbf{v}-\mathbf{V}|}{v+V}\ . \tag{4}$$

This equation is used to calculate probabilities of sampling from the first or second PDF inside the square brackets in Eq. (4):

$$P_1 = \frac{N\sigma_s v}{D(v)} \ , \ P_2 = \frac{2N\sigma_s}{\sqrt{\pi\alpha_s}\ D(v)} \ , \ D(v) = N\sigma_s v + \frac{2N\sigma_s}{\sqrt{\pi\alpha_s}} \ .$$

Using this information, the rejection technique is introduced.

3.1 Free Gas Scattering Algorithm

H. Kahn [1] first proposed the free gas scattering algorithm and this algorithm was adapted into MCNP to form the free gas scattering kernel. In MCNP5 source code, the free gas scattering kernel resides in the subroutine tgtvel.F90. Conditions that determine the use of the free gas scattering kernel in tgtvel.F90 are specified in colidn.F90. Kahn's original algorithm is depicted in Fig. 1.

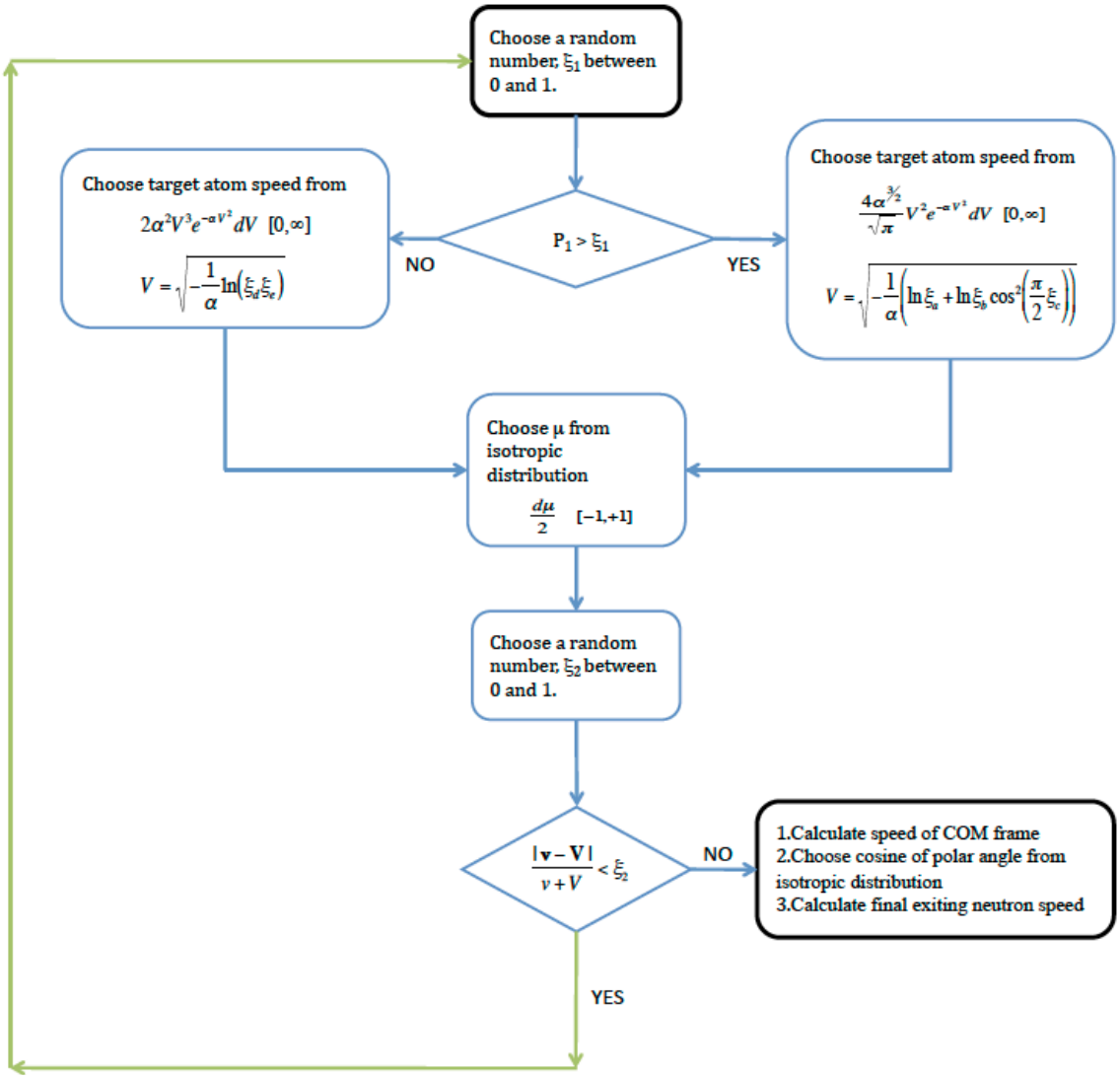

*Note: ξ_I represents a random number that ranges from 0 to 1

Figure 1: Free gas Scattering Algorithm [1]

A test is conducted to determine the Maxwell-Boltzmann distribution from which the target atom speed will be selected. Based on the probability test, the target atom speed is chosen from $2\alpha^2 V^3 e^{-\alpha V^2} dV$ or $4\alpha^{3/2}/\sqrt{\pi} V^2 e^{-\alpha V^2} dV$. Once the speed of the target atom has been selected, the cosine of polar angle between the neutron and target atom is determined from an isotropic distribution since scattering is considered isotropic in the Center-of-Mass (COM) frame. The choice of the two parameters, target atom speed and cosine of polar angle, are then tested using a rejection technique based on the ratio of the relative speed of the neutron and the sum of the speeds of the neutron and the target atom. If the two choices pass the rejection test, then the speed of the COM frame is calculated along with a random selection of the cosine of polar angle of the exiting neutron, which is once again selected from an isotropic distribution. All these variables can be now used to determine the final exiting speed of the neutron in laboratory frame.

MCNP does not directly sample from $4\alpha^{3/2}/\sqrt{\pi} V^2 e^{-\alpha V^2} dV$. Instead, a rejection technique has been implemented to sample from this distribution. This is because direct sampling involves calculating logarithmic and cosine functions and this was computationally expensive before the days of supercomputers. However, the computational expense of processing cosine and logarithmic functions is now significantly smaller and this can be easily changed in MCNP.

In MCNP, absorption is taken into account through the method of implicit capture where the neutron is assigned a weight. A history begins with a neutron weight of one and with each scatter the neutron weight is multiplied by the ratio of scattering cross section to total cross section.

$$w_{i+1} = w_i \left(1 - \frac{\sigma_{capture}}{\sigma_{total}}\right). \quad (5)$$

After a neutron weight falls below a specific weight window, it undergoes a Russian roulette process, which results in increased particle weight or particle termination.

3.1.1 Drawbacks of Current Method

There are some drawbacks to the current method that are more significant in reactor calculations that involve VHTRs and LWRs as a result of assuming constant scattering cross sections in the epithermal range when it is not the case for heavy nuclides like U-238 as seen in Fig. 3. The assumption of using constant scattering cross sections is valid for moderation of neutrons from light nuclides since the cross sections stay nearly constant in the epithermal range. The assumption of using constant cross sections even for heavy nuclides is often justified because moderation of a neutron by a heavy nuclide is typically negligible and therefore, the effects of resonances in these nuclides are ignored. However, this is not the case because neutrons can gain or lose enough energy when scattering off these heavy nuclides to fall into an absorption resonance.

The change in scattering cross section in the epithermal range has to be taken into account, especially for U-238 in reactor applications since it is considered to affect criticality calculations on the order of several hundred pcm depending on the temperature and packing fraction of the fuel.

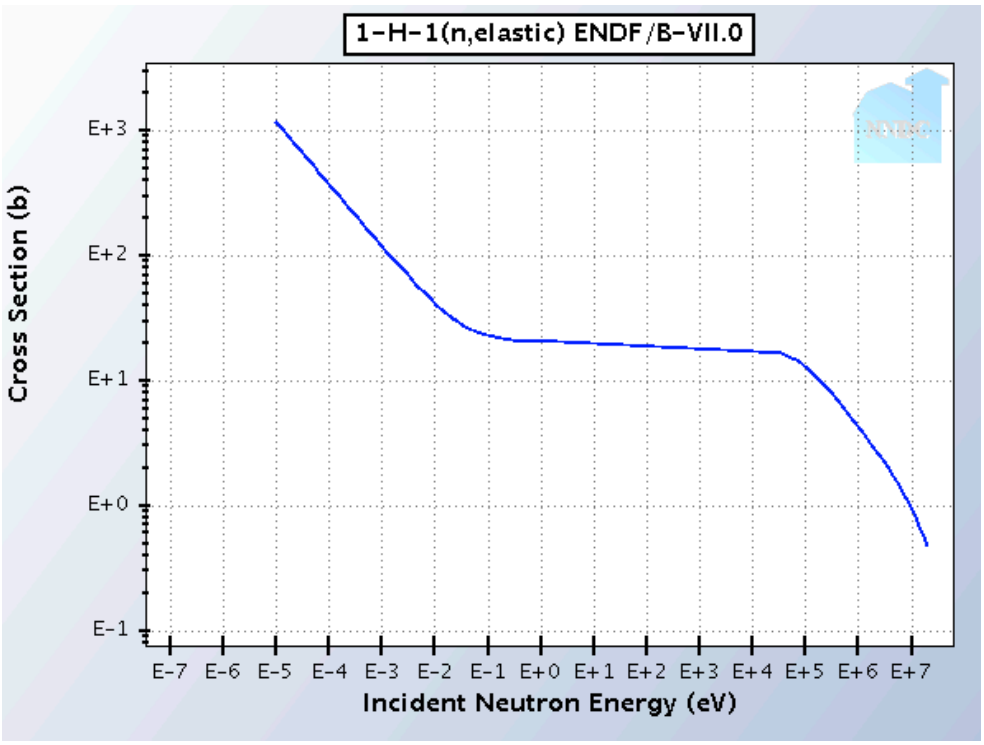

Figure 2: 1-H-1 Elastic Scattering Cross Section at 300K [10]

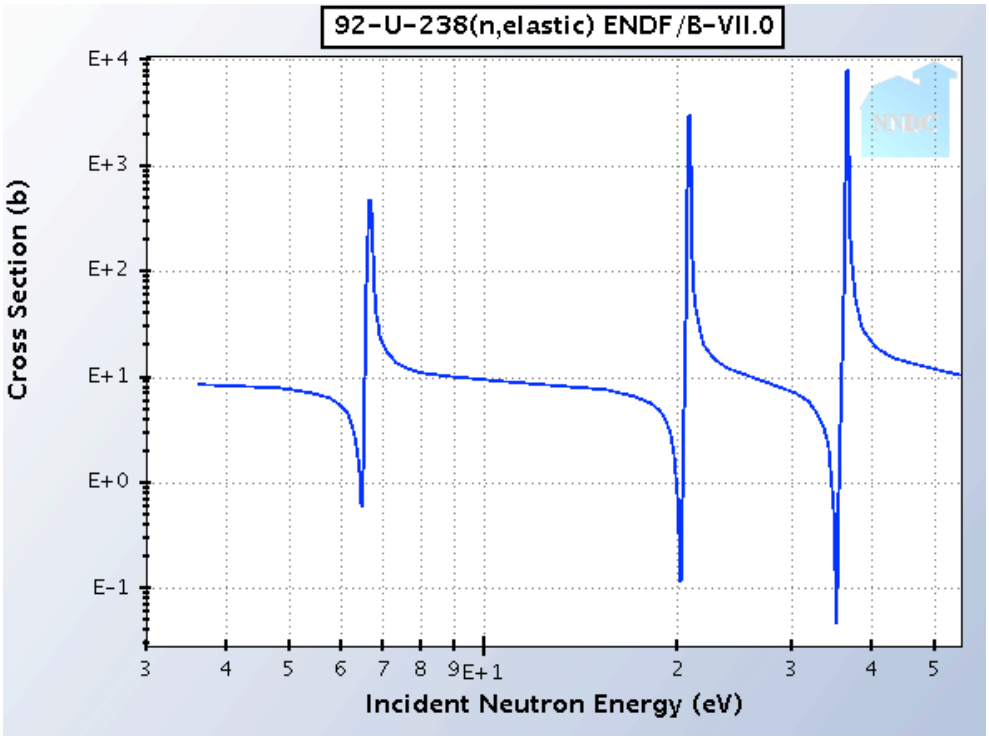

Figure 3: U-238 Elastic Scattering Cross Section at 300K [10]

3.2 Doppler Broadening Rejection Correction (DBRC) Method

B. Becker *et. al.* [5] developed and implemented a scheme to account for the change in scattering cross sections due to low-lying resonances in the epithermal range by modifying the existing free gas scattering kernel.

The original free gas algorithm remains intact except for an additional constraint based on scattering cross sections, which is not assumed to be constant in the DBRC method. This additional constraint is shown in Eq. (6). It is the ratio of the zero Kelvin scattering cross section for the relative neutron speed and the maximum zero Kelvin scattering cross section for a specific range, E_ε,

$$P(V,\mu|v)dV\,d\mu = \frac{1}{\sum_{eff,s}(v)} \begin{bmatrix} 4\pi N\left(\frac{\alpha}{\pi}\right)^{3/2} vV^2 e^{-\alpha V^2} dV \frac{d\mu}{2} + \ldots \\ \ldots 4\pi N\left(\frac{\alpha}{\pi}\right)^{3/2} V^3 e^{-\alpha V^2} dV \frac{d\mu}{2} \end{bmatrix} \left(\frac{|\mathbf{v}-\mathbf{V}|}{v+V}\right) \left(\frac{\sigma(E_r,0)}{\sigma_{\max}(E_\varepsilon,0)}\right). \quad (6)$$

where E_r is the relative neutron energy and E_ε is the energy range in which the maximum scattering cross section is determined. ε is a dimensionless variable that equates to $\sqrt{AE/kT}$ and ranges from ± 4.0, where E is the incident neutron energy. The following steps establish the energy interval, E_ε:

$$\sqrt{\frac{AE}{kT}} + 4 = \sqrt{\frac{AE_{\max}}{kT}},$$

$$E_{\max} = \frac{kT}{A}\left(\sqrt{\frac{AE}{kT}} + 4\right)^2. \quad (7)$$

$$\sqrt{\frac{AE}{kT}} - 4 = \sqrt{\frac{AE_{\min}}{kT}},$$

$$E_{\min} = \frac{kT}{A}\left(\sqrt{\frac{AE}{kT}} - 4\right)^2. \quad (8)$$

Here,

$$E_\varepsilon = E_{\max} - E_{\min}. \quad (9)$$

As described in the previous section, the rejection scheme is developed from the constraints formulated from the reaction rate equation below. The algorithm for DBRC is presented in Fig. 4.

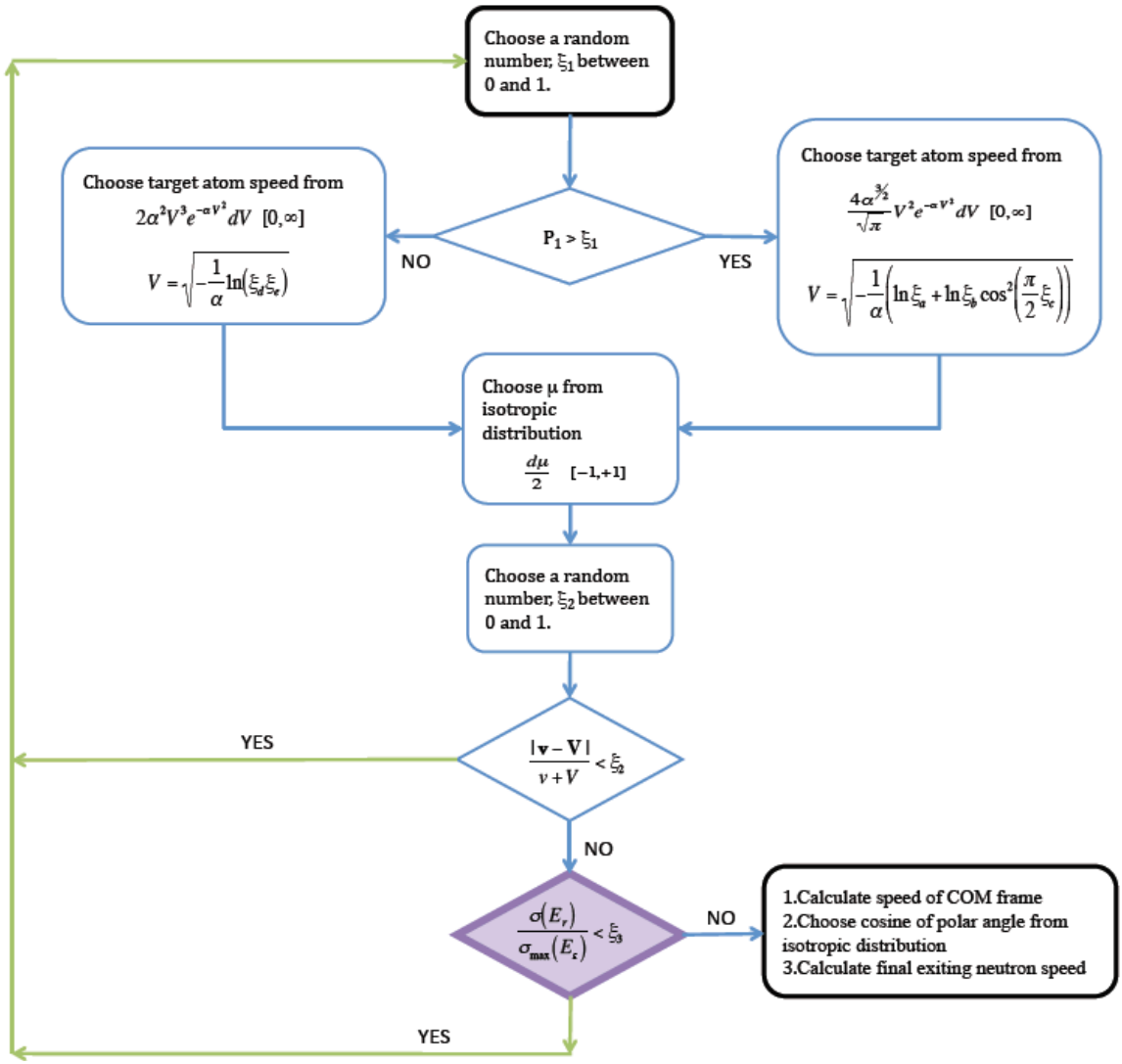

*Note: ξ_I represents a random number that ranges from 0 to 1

Figure 4: DBRC Algorithm proposed by B. Becker *et. al.* [5] [11]

After the speed of the target atom and cosine of polar angle have been selected and the two variables have passed the first rejection test, the choices made for the target atom speed and angle are not accepted yet as it would be in the original free gas scattering algorithm. Becker and Dagan proposed the implementation of a second rejection test, where the two variables, atom speed and angle, are tested against the ratio of the cross sections in the range for E_ε corresponding to specific incident neutron energies.

4 MCNP5 WITH DBRC

A separate module was created to contain all the calculations that are required to make the scattering decision regarding target atom speed and cosine of polar angle between the neutron and atom. This module contains a function that determines the decision of the second rejection test and a subroutine that reads in all the zero Kelvin scattering cross section values for U-238. It also contains subroutines that use the target atom speed and cosine of polar angle selected in tgtvel.F90 to determine, E_ε, for specific incident neutron energies.

Next, the corresponding maximum cross section value in the energy range, E_ε, and the scattering cross section for the relative neutron speed are determined which is then finally used to determine the decision of the second rejection test. The upper energy limit that activates the use of free gas scattering kernel is set in colidn.F90. This energy limit is set to 210 eV as recommended by B. Becker in his thesis [11].

4.1 Comparison of Double-Differential Scattering Kernels

The double-differential scattering kernel produced by the original free gas scattering kernel in MCNP does take into account neutron up-scattering. However, it does not produce the true double-differential scattering kernel because of the simplifying assumption of using constant scattering cross sections in epithermal region for heavy nuclides. When resonance scattering is taken into account by using cross sections dependent on relative neutron speed in the free gas scattering kernel, the true double-differential scattering kernel can be found to represent correct neutron scattering behavior. Fig. 5 shows the difference in up-scattering effects in the original free gas scattering kernel in MCNP and the modified free gas scattering kernel that accounts for resonance scattering.

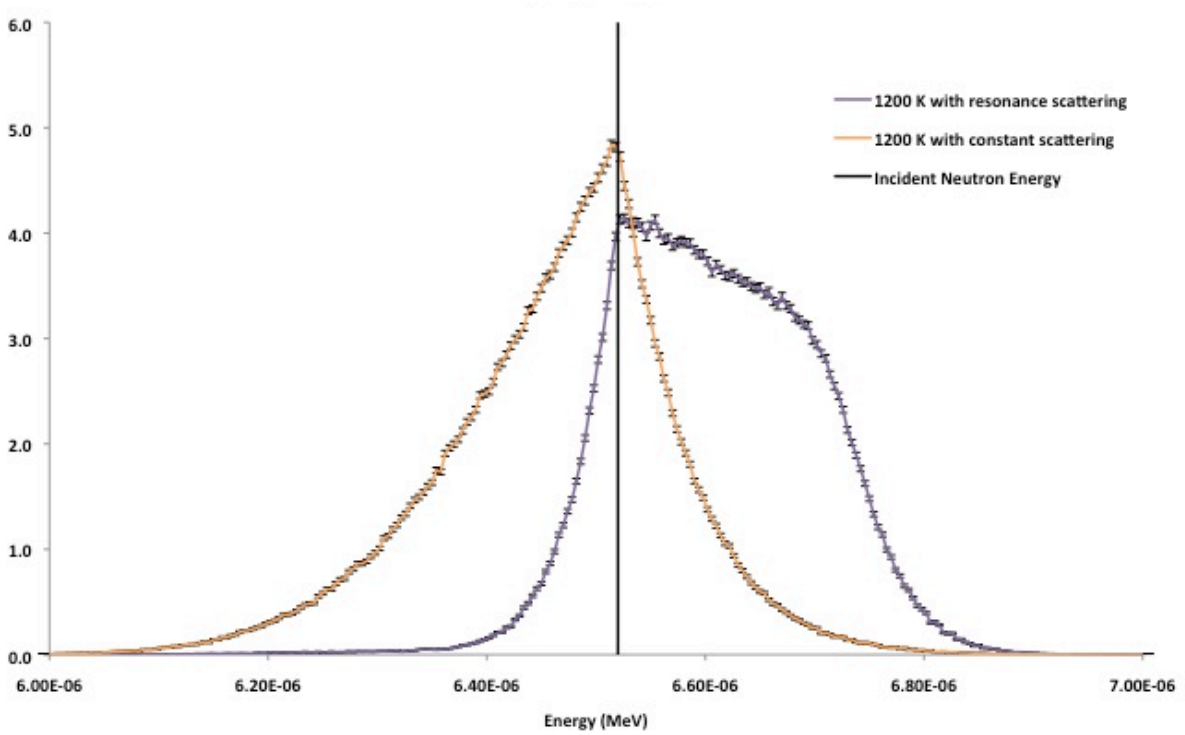

Figure 5: Comparison of Double-Differential Scattering Kernels for U-238 at 1200 K for Incident Neutron Energy of 6.52 eV

Fig. 5 illustrates how the up-scattering percentage for just this resonance in U-238 is significantly underestimated by assuming constant scattering cross sections for heavy nuclides in the epithermal region in the original free gas scattering kernel. This suggests that up-scattering percentages are significantly underestimated for specific neutron energies around low-lying resonance energies in the epithermal region for heavy nuclides.

4.2 Temperature Effects on Double-Differential Scattering Kernel

The scattering kernel is a function of temperature and up-scattering percentages increase as the temperature of the target material increases. Fig. 6 shows how the double-differential scattering kernel changes as a function of temperature.

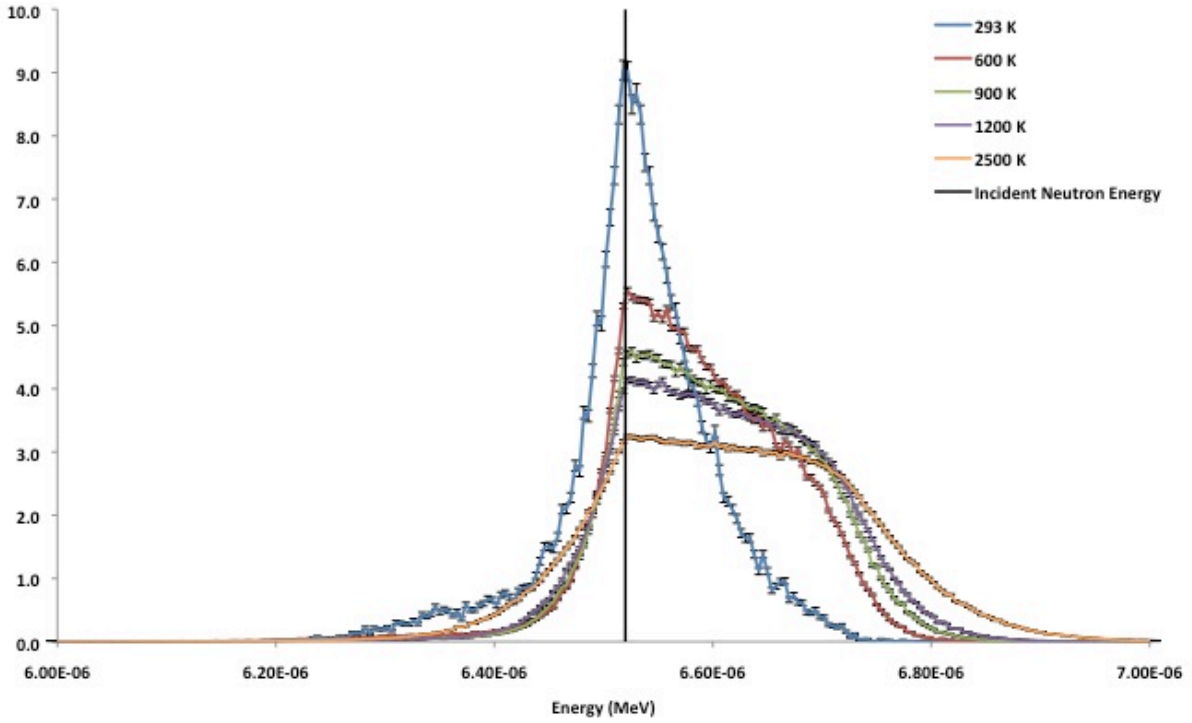

Figure 6: Scattering Kernel for U-238 at Varying Temperatures for Incident Neutron Energy of 6.52 eV

For benchmarking purposes, the up-scattering percentages were calculated for specific incident neutron energies around low-lying resonances in U-238 and these values are compared to values obtained by Ouisloumen *et. al.* [3] and D. Lee *et. al*. [6].

Table I: Up-scatter Percentages for Varying Incident Neutron Energies for U-238 at 1000K

Resonance (eV)	Neutron Energy (eV)	Ouisloumen *et. al.* Results [3]	D. Lee *et. al.* Results [6] (1 σ std. dev)	Modified MCNP5 Results (1 σ std. dev)
6.67	6.52	82.03	83.40 (0.04)	83.64 (0.19)
	7.20	28.12	28.20 (0.01)	28.03 (0.05)
36.67	36.25	54.23	55.28 (0.06)	53.69 (0.01)
	37.20	7.95	7.26 (0.01)	7.72 (0.02)

The results show that the up-scattering percentages from modified MCNP5 compares very well with results obtained through different methods developed by Ouisloumen *et. al.* [3] and D. Lee *et. al* [6].

4.3 Mosteller Benchmark Problem

The Mosteller benchmark problem [12], [13] for LWR pin cell with UO_2 fuel is chosen to benchmark MCNP5 results with resonance scattering to the results published in [6] and [9]. ENDF/B-VII.0 cross sections are used for this calculation and zirconium isotope abundances for natural zirconium are obtained from NIST [14] and used as weight fractions for pure zirconium in the benchmark problem.

Table II: Natural Zirconium Isotope Abundances [14]

	Abundance (%)
Zr-90	51.45
Zr-91	11.22
Zr-92	17.15
Zr-94	17.38
Zr-96	2.8

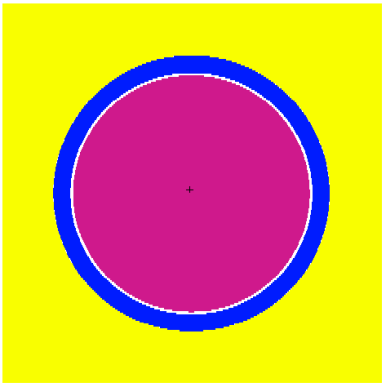

Figure 7: LWR Pin Cell in Mosteller Benchmark [12]

The MCNP5 setup in Fig. 5 shows the LWR pin cell that was modeled in Mosteller benchmark problems.

In order to calculate the Fuel Temperature Coefficient (FTC), two sets of calculations are done in MCNP5. The first is at Hot Zero Power (HZP) conditions where the fuel, cladding and moderator are set at a temperature of 600K. The second set of calculations is done under Hot Full Power (HFP) conditions where the fuel temperature is set at 900K and the cladding and moderator temperatures are at 600K.

FTC is calculated using,

$$FTC = \left(\frac{1}{k_{HZP}} - \frac{1}{k_{HFP}} \right) \times \frac{10^5}{\Delta T}, \qquad (10)$$

where ΔT is 300K.

The results obtained from this benchmark exercise are comparable to those presented in [6] and [9]. The FTC decreased after resonance scattering is taken into account. MCNP5 results with constant free gas scattering are presented in Table 3.

Table III: MCNP5 k_{eff} Results with Constant Free Gas Scattering

wt%	k_{eff} at HZP			k_{eff} at HFP			FTC (pcm/K)		
0.711	0.66569	±	0.00019	0.65987	±	0.00020	-4.42	±	0.21
1.6	0.96124	±	0.00026	0.95295	±	0.00025	-3.02	±	0.13
2.4	1.09913	±	0.00026	1.08986	±	0.00029	-2.58	±	0.11
3.1	1.17657	±	0.00030	1.16777	±	0.00027	-2.13	±	0.10
3.9	1.23944	±	0.00028	1.23009	±	0.00027	-2.04	±	0.09
4.5	1.27495	±	0.00032	1.26542	±	0.00027	-1.97	±	0.09
5.0	1.29920	±	0.00034	1.28911	±	0.00029	-2.01	±	0.09

Table 4 shows results obtained when resonance free gas scattering is taken into account. FTC for 4.5 wt% U-235 looks slightly higher than those at 3.9 wt% and 5.0 wt% due to statistical fluctuations. An independent check on the FTC was conducted using the same code and the values for FTCs are comparable to results

presented in [6] and [9]. This leads to the conclusion that the FTCs oscillate due to statistical fluctuations unavoidable in Monte Carlo methods and as the number of particles and cycles are increased, the FTCs become more stable.

Table IV: MCNP5 k_{eff} Results with Resonance Free Gas Scattering

wt%	k_{eff} at HZP			k_{eff} at HFP			FTC (pcm/K)		
0.711	0.66541	±	0.00022	0.65909	±	0.00020	-4.80	±	0.23
1.6	0.96044	±	0.00026	0.95142	±	0.00022	-3.29	±	0.12
2.4	1.09889	±	0.00027	1.08877	±	0.00029	-2.82	±	0.11
3.1	1.17613	±	0.00026	1.16563	±	0.00028	-2.55	±	0.09
3.9	1.23924	±	0.00029	1.22866	±	0.00030	-2.32	±	0.09
4.5	1.27460	±	0.00025	1.26271	±	0.00031	-2.46	±	0.08
5.0	1.29860	±	0.00029	1.28748	±	0.00030	-2.22	±	0.08

The results show that FTCs decrease as expected when resonance free gas scattering is taken into account. Fig. 8 illustrates the difference in Doppler coefficients computed in MCNP5 with constant and resonance free gas scattering models. The figure depicts the negative shift in FTC due to resonance scattering due to the greater likelihood of losing a neutron as they gain energy and fall into an absorption resonance in the epithermal range.

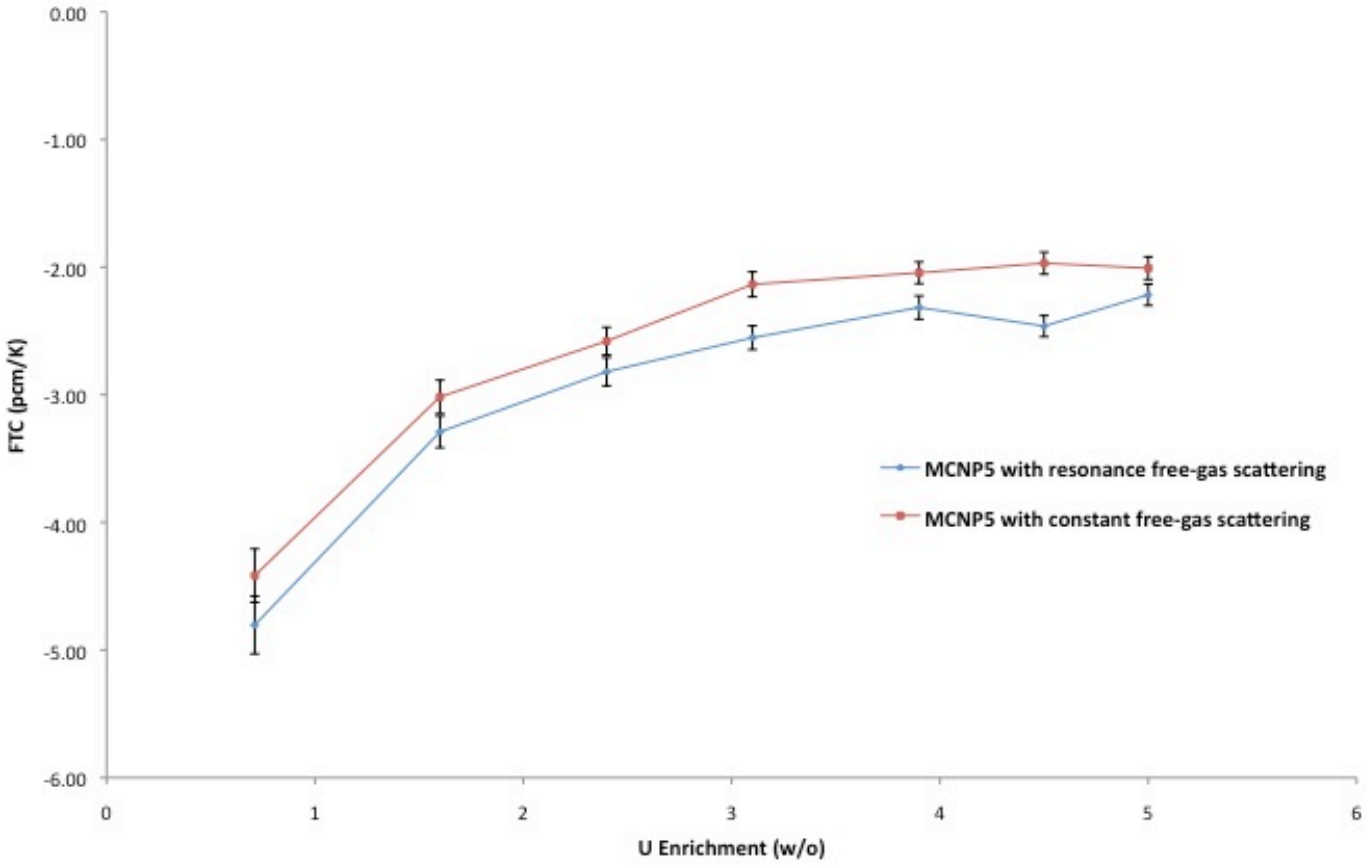

Figure 8: FTCs for UO_2 Pin Cell (LWR)

Table 5 shows the difference in k_{eff} increases with fuel temperature due to resonance scattering. The difference is on the order of several hundred pcm for LWR pin cell calculations at full power. This clearly shows that resonance scattering cannot be ignored in full power reactor calculations for LWRs and VHTRs.

Table V: Difference in k_{eff} due to Resonance Free Gas Scattering

wt%	HZP (pcm)	HFP (pcm)
0.711	-28 ± 29	-78 ± 28
1.6	-80 ± 37	-153 ± 33
2.4	-24 ± 37	-109 ± 41
3.1	-44 ± 40	-214 ± 39
3.9	-20 ± 40	-143 ± 40
4.5	-35 ± 41	-271 ± 41
5.0	-60 ± 45	-163 ± 42

4.3.1 Computational Time Study

A study on computational time was conducted for criticality calculations with resonance scattering in free gas for energies below 210 eV. The time it takes to run these criticality problems increased as temperature of the fuel increased. Table VI shows that there is over a 10% increase in computational time for HFP cases and about 6 – 9 % increase in computational time for HZP cases.

Table VI: Time difference (%) between Standard and Modified MCNP5

	TIME DIFFERENCE (%)	
wt%	**HZP**	**HFP**
0.711	6.45	10.47
3.1	9.17	13.13
5.0	6.09	11.56

4.4 Energy Limits for Resonance Free Gas Scattering

A study was conducted on FTC behavior when the upper energy limit at which resonance free gas scattering invoked is changed. The results from this parametric study on varying energy limits for free gas scattering is presented in Table 7.

Table VII: k_{eff} due to varying energy limits for resonance free gas scattering

Energy Limit (eV)	**50**	**90**	**150**	**210**	**250**	**500**	**1000**
wt%	**FTC (pcm/K)**	**FTC (pcm/K)**	**FTC (pcm/K)**	**FTC (pcm/K)**	**FTC (pcm/K)**	**FTC (pcm/K)**	**FTC (pcm/K)**
0.711	-5.11 ± 0.22	-4.88 ± 0.20	-4.90 ± 0.20	-4.80 ± 0.23	-4.91 ± 0.21	-4.66 ± 0.21	-4.90 ± 0.20
3.1	-2.60 ± 0.10	-2.60 ± 0.09	-2.72 ± 0.09	-2.55 ± 0.09	-2.67 ± 0.10	-2.62 ± 0.11	-2.57 ± 0.10
5.0	-2.20 ± 0.08	-2.34 ± 0.08	-2.28 ± 0.08	-2.22 ± 0.08	-2.26 ± 0.09	-2.23 ± 0.08	-2.29 ± 0.08

The results show that FTCs oscillate around similar values after the upper energy limit was set above 50 eV. However, for 500 eV, FTC for 0.711 wt% U is slightly lower than other cases, however, the value is reasonable since it is within two standard deviations of the corresponding results above 50 eV upper limit. This suggests that there is no need to invoke the modified free gas scattering kernel for the entire epithermal region in U-

238. However, these upper limits will be different for other nuclides since the energies at which their resonance lie are different and neutron up-scattering percentages will vary accordingly.

4.5 MCNP Extended Criticality Validation Suite

The MCNP Extended Criticality Validation Suite is run with constant free gas scattering in MCNP5 and with resonance free gas scattering below 210 eV in modified MCNP5. The Extended Criticality Validation Suite contains 119 problems from ICSBEP Handbook out of which only less than ten problems contain low-enriched uranium. Therefore, the difference in criticality calculations is insignificant because of the nature of problems in the benchmark suite and the temperatures for the benchmark problems, which are at 300K. Resonance free gas scattering is not expected to affect criticality calculations significantly at this temperature and the benchmark calculations validated the expectations.

4.6 Resonance Scattering Effects on Criticality and Safety Studies

Resonance scattering is expected to affect criticality and safety studies for only very specific problems, namely those that involve high-temperature calculations. Criticality calculations vary on the order of only 10 pcm for reactor calculations at room temperature and this suggests that resonance scattering does not make a considerable difference to criticality calculations at room temperature. Table V shows that for temperature of the fuel at 600 K for HZP LWR pin cell calculations, k_{eff} in criticality calculations is reduced by approximately 40 pcm, which is not a significant change. However, under HFP conditions where the fuel is at 900 K, k_{eff} is reduced by approximately 150 pcm. This reduction in k_{eff} leads to a negative shift in FTCs as shown in Table IV. These criticality calculations for LWR pin cells using the modified resonance free gas scattering model show that k_{eff} does not change considerably in LWRs unless full power criticality studies are being performed.

However, HFP and HZP temperature conditions in a VHTR are much higher than those for LWRs, and as seen in Fig. 6 in the double-differential scattering kernel for 1200 K and 2500 K, the up-scattering percentages for neutrons scattering off U-238 are higher than they are at 900 K or lower. Studies by D. Lee *et. al.* [6] shows k_{eff} reduction on the order of 400 pcm in VHTRs, which is significant. As a result, criticality and safety studies using resonance scattering in the free gas scattering kernel is expected to affect VHTR criticality analysis more so than LWR criticality and safety studies. This suggests that criticality and safety studies involving VHTRs should use this modified free gas scattering model that includes resonance scattering in U-238.

5 CONCLUSION AND FUTURE WORK

The DBRC method developed by Becker *et. al.* [5] is correctly implemented in MCNP5-1.60. Only high-temperature applications are affected by this modification and models at room temperature are not expected to change. For VHTR and LWR criticality calculations, this modification can change k_{eff} on the order of several hundred pcm. However, there is no need to invoke the modified free gas scattering kernel for the entire epithermal region. Future work should focus on determining nuclides for which the modified free gas scattering kernel needs to be implemented and the upper energy limits at which it is invoked for these nuclides. An investigation into significance of up-scattering percentages for low-lying resonances in various nuclides needs to be conducted so that the modified free gas scattering kernel can be applied to broader applications.

REFERENCES

1. R. R. Coveyou, R. R. Bate & R. K. Osborn, "Effect of Moderator Temperature Upon Neutron Flux In Infinite, Capturing Medium," *Journal of Nuclear Energy,* **2**, pp. 153-167 (1956).
2. X-5 Monte Carlo Team, "MCNP – A General Monte Carlo N-Particle Transport Code, Version 5, Volume I: Overview and Theory," LA-UR-03-1987, *Los Alamos National Laboratory* (2003).
3. M. Ouisloumen & R. Sanchez, "A Model for Neutron Scattering Off Heavy Isotopes That Accounts for Thermal Agitation Effects," *Nuclear Science and Engineering,* **107**, pp. 189-200 (1991).
4. W. Rothenstein & R. Dagan, "Ideal gas scattering kernel for energy dependent cross section," *Annals of Nuclear Energy*, **25**, pp. 209 – 222 (1998).
5. B. Becker, R. Dagan & G. Lohnert, "Proof and implementation of the stochastic formula for ideal gas, energy dependent scattering kernel," *Annals of Nuclear Energy*, **36**, pp. 470 – 474 (2009).
6. D. Lee, K. Smith & J. Rhodes, "The impact of ^{238}U resonance elastic scattering approximations on thermal reactor Doppler reactivity," *Annals of Nuclear Energy,* **36**, pp. 274-280 (2009).
7. G. J. Marchuk, V. G. Turchin, V. N. Smelov & G. A. Il'yasova, *Proceedings from Brookhaven Conference on Neutron Thermalization*, **II**, pp. 706 (1962).
8. G. L. Blackshaw & R. L. Murray, "Scattering Functions for Low-Energy Neutron Collisions in a Maxwellian Monatomic Gas," *Nuclear Science and Engineering*, **27**, pp. 520-532 (1967).
9. T. Mori & Y. Nagaya, "Comparison of Resonance Elastic Scattering Models Newly Implemented in MVP Continuous-Energy Monte Carlo Code," *Journal of Nuclear Science and Technology,* Vol 46, No. 8, pp. 793-798 (2009).
10. National Nuclear Data Center, *Evalulated Nuclear Data File (ENDF) Retrieval & Plotting, Library: ENDF/B-VII.0 (2006).*
11. B. Becker, "On the Influence of the Resonance Scattering Treatment in Monte Carlo Codes on High Temperature Reactor Characteristics," Thesis, *Institut fur Kernenergetik und Energiesysteme, Germany*, 2010.
12. R. D. Mosteller, "Computational Benchmarks for the Doppler Reactivity Defect," *LA-UR-06-2968, Los Alamos National Laboratory*.
13. R. D. Mosteller, "ENDF/B-V, ENDF/B-VI, and ENDF/B-VII.0 Results for the Doppler-defect Benchmark," *Proceedings from M&C+SNA,* Monterey, CA (2007).
14. National Institute of Standards and Technology, "Atomic Data for Zirconium (Zr)," *Handbook of Basic Atomic Spectroscopic Data – online version* (2011).